IL-15 is a component of the inflammatory milieu in the tumor microenvironment promoting antitumor responses

Rosa M. Santana Carrero[a,b], Figen Beceren-Braun[b], Sarai C. Rivas[b], Shweta M. Hegde[b], Achintyan Gangadharan[b], Devin Plote[b,c], Gabriel Pham[b], Scott M. Anthony[a,b,1], and Kimberly S. Schluns[a,b,2]

[a]Immunology Graduate Program, University of Texas (UT) MD Anderson Cancer Center UTHealth Graduate School of Biomedical Sciences, Houston, TX 77584; [b]Department of Immunology, University of Texas MD Anderson Cancer Center, Houston, TX 77584; and [c]Cancer Biology Graduate Program, University of Texas MD Anderson Cancer Center UTHealth Graduate School of Biomedical Sciences, Houston, TX 77584

Edited by Averil Ma, University of California, San Francisco, CA, and accepted by Editorial Board Member Philippa Marrack November 30, 2018 (received for review August 28, 2018)

Previous studies have provided evidence that IL-15 expression within human tumors is crucial for optimal antitumor responses; however, the regulation of IL-15 within the tumor microenvironment (TME) is unclear. We report herein, in analyses of mice implanted with various tumor cell lines, soluble IL-15/IL-15Rα complexes (sIL-15 complexes) are abundant in the interstitial fluid of tumors with expression preceding the infiltration of tumor-infiltrating lymphocytes. Moreover, IL-15 as well as type I IFN, which regulates IL-15, was required for establishing normal numbers of CD8 T cells and natural killer cells in tumors. Depending on tumor type, both the tumor and the stroma are sources of sIL-15 complexes. In analyses of IL-15 reporter mice, most myeloid cells in the TME express IL-15 with CD11b^{+}Ly6C^{hi} cells being the most abundant, indicating there is a large source of IL-15 protein in tumors that lies sequestered within the tumor stroma. Despite the abundance of IL-15–expressing cells, the relative levels of sIL-15 complexes are low in advanced tumors but can be up-regulated by local stimulator of IFN genes (STING) activation. Furthermore, while treatment of tumors with STING agonists leads to tumor regression, optimal STING-mediated immunity and regression of distant secondary tumors required IL-15 expression. Overall, our study reveals the dynamic regulation of IL-15 in the TME and its importance in antitumor immunity. These findings provide insight into an unappreciated attribute of the tumor landscape that contributes to antitumor immunity, which can be manipulated therapeutically to enhance antitumor responses.

interleukin 15 | tumors | CD8 T cells | myeloid cells | interferons

Patients vary considerably in their responses to cancer therapies. The presence of tumor-infiltrating T cells strongly correlates with positive clinical outcomes in melanoma, colon, breast, cervical, and brain cancers (1–4). Specifically, the density, depth, and functional attributes of cytolytic CD8 T cells are associated with the greatest clinical outcomes (1). Altogether, these features are a better prognostic indicator than the tumor–node–metastasis classification that is currently used. IL-15 is a cytokine that preferentially stimulates CD8 T cell and natural killer (NK) cell activation, proliferation, and cytolytic activity. Not surprisingly, these functional activities of IL-15 translate to enhanced antitumor responses in multiple tumor models (5–7). As such, systemic treatments with IL-15 or IL-15 analogs are currently being evaluated as potential cancer therapeutics. In addition to the ability of IL-15 to act systemically to promote antitumor responses, there is evidence that IL-15 expression within the tumor microenvironment (TME) is crucial for optimal antitumor responses (8, 9). Galon and coworkers showed that loss of IL-15 expression within colorectal tumors correlated with lower T cell density, decreased T cell proliferation, higher risk of relapse, and decreased survival (8). While these studies suggest IL-15 produced within the TME is important for effective antitumor responses by CD8 T cells, the mechanisms regulating IL-15 within tumors are unknown.

IL-15 has a unique form of expression whereby it associates with the IL-15Rα protein intracellularly and is shuttled to the cell surface as a complex (10, 11). This cell surface complex of IL-15 and IL-15Rα efficiently stimulates neighboring cells via the IL-2/15Rβ and γC complex via the mechanism of transpresentation (10). Previous studies have provided evidence that transpresentation mediates IL-15 responses during homeostasis (12–14). Interestingly, IL-15Rα/IL-15 complexes are cleaved from the cell surface, which generates transient but significant increases in soluble IL-15Rα/IL-15 complexes (sIL-15 complexes) in response to numerous types of immune stimulation (15, 16). Specifically, sIL-15 complexes are induced by total body irradiation, TLR stimulation, virus infections, CD40 stimulation, type I IFNs (IFN-I), and most recently activation of the stimulator of IFN genes (STING) pathway (15–18). sIL-15 complexes produced upon immune activation could be mediators of IL-15 responses as recombinant sIL-15 complexes are 50–100 times more potent than rIL-15 in promoting CD8

Significance

Expression and regulation of IL-15 in the tumor microenvironment are poorly understood and are important as studies have provided correlative data that IL-15 expression within human tumors is a critical factor dictating antitumor responses. Moreover, IL-15 utilizes unique mechanisms that preclude typical expression analyses. Herein we demonstrate using multiple tumor models that soluble (s) IL-15/IL-15Rα complexes are expressed in tumors and regulate tumor-infiltrating lymphocyte numbers. While the levels of sIL-15 complexes are low in established tumors, IL-15–expressing myeloid cells are abundant. Nonetheless, providing a local inflammatory signal upregulates sIL-15 complexes within the tumor and drives tumor regression in an IL-15–dependent manner. Thus, our findings reveal a strategy for unleashing a natural resource within tumors that enhances antitumor responses.

Author contributions: K.S.S. designed research; R.M.S.C., F.B.-B., S.C.R., S.M.H., A.G., D.P., G.P., S.M.A., and K.S.S. performed research; R.M.S.C., F.B.-B., G.P., S.M.A., and K.S.S. analyzed data; and R.M.S.C., S.M.A., and K.S.S. wrote the paper.

The authors declare no conflict of interest.

This article is a PNAS Direct Submission. A.M. is a guest editor invited by the Editorial Board.

[1]Present address: Department of Microbiology and Immunology, University of Iowa, Iowa City, IA 52242.

[2]To whom correspondence should be addressed. Email: kschluns@mdanderson.org.

This article contains supporting information online at www.pnas.org/lookup/suppl/doi:10.1073/pnas.1814642116/-/DCSupplemental.

Published online December 26, 2018.

T cell and NK cell proliferation in vivo (19, 20). Nonetheless, while definitive evidence is lacking that native sIL-15 complexes produced in vivo are stimulatory, increases in in vivo sIL-15 complexes coincide with increases in IL-15–dependent CD8 T cell proliferation (16, 18). Hence, unlike transpresentation, the production of sIL-15 complexes represents a mechanism inducing IL-15 responses that is not dependent on the formation of a cell–cell interaction.

Identifying the cellular sources of IL-15 has been challenging as the detection of IL-15 protein has been difficult. These difficulties are due in part to the low levels of IL-15 present on the cell surface, the sequestering of IL-15 to the cell surface by IL-15Rα, and possibly the inability to detect IL-15 complexed to the IL-15Rα. Nonetheless, studies using models that restrict IL-15 expression to specific cell types have provided evidence that numerous cell types are important sources for IL-15, including macrophages, dendritic cells (DCs), intestinal epithelial cells, thymic epithelial cells, and keratinocytes (12–14, 21–26). Recently, IL-15 expression among different cell types has been better defined in studies using IL-15 reporter mice. Two different lines of IL-15 reporter mice have been described: (*i*) transcriptional IL-15 reporter (27, 28) and (*ii*) translational IL-15 reporter (29). The transcriptional reporter line was generated with a BAC transgene that inserted EGFP downstream of the IL-15 promoter, wherein GFP expression reflects the activity of the IL-15 promoter. The translational reporter line utilized a BAC transgene that inserted a GFP downstream of the IL-15 gene that leads to expression of both the IL-15 protein in conjunction with GFP protein that remains in the cell after cleavage. While the GFP reflects the amount of IL-15 protein produced by the cell, the GFP does not mimic the transport of IL-15. Therefore, a caveat of these models is the inability to identify cells transpresenting IL-15 on the surface or those producing sIL-15 complexes. Regardless of the differences in how these two lines were generated, the IL-15 expression profiles are virtually the same in the IL-15 transcriptional and translational reporter mice (27–29). In analysis of the IL-15 transcriptional reporter mice, expression of IL-15 displayed hierarchical expression among myeloid cells, with basophils > eosinophils/mast cells > neutrophils/monocytes > $CD8^+$ DCs > macrophages > $CD11c^+$ DCs (27). This IL-15 reporter expression is present during the steady state and up-regulated in specific cell types after virus infection or total body irradiation (18, 27, 28).

With the clear importance of IL-15 in enhancing antitumor responses, we set out to examine the extent to which IL-15 is expressed within the TME, the form in which IL-15 is expressed, the cellular source, the mechanisms regulating IL-15, and its effects on tumor-infiltrating lymphocytes (TILs). This present study demonstrates that IL-15 is expressed in the TME as sIL-15 complexes and regulates TIL numbers. sIL-15 complexes are abundant in early tumors but low in established tumors, even though IL-15–expressing cells are abundant in established tumors. Nonetheless, sIL-15 complexes can be up-regulated by stimulating the inflammatory STING pathway. More importantly, the induction of IL-15 expression by locally delivered inflammatory signals was critical for mediating antitumor responses.

Results

IL-15 Is Expressed in the Tumor Microenvironment as sIL-15 Complexes and Regulates Tumor-Infiltrating Lymphocyte Numbers. There is an emerging paradigm that the TME initially produces inflammatory mediators, which promote antitumor responses but then gradually converts to an immunosuppressive environment (30, 31). Our findings that sIL-15 complexes are produced in response to numerous forms of immune stimulation compelled us to investigate whether sIL-15 complexes are produced in the TME. To determine if sIL-15 complexes are produced in B16 melanoma tumors, B16 tumors (B16-F10) were established in wild-type (WT) C57BL/6 mice, removed along with spleens, measured in size and weight (tumor weight between 20 and 150 mg), dissociated, and suspended in PBS. Supernatants generated after pelleting cells were analyzed for sIL-15 complexes using ELISA. We found that sIL-15 complexes were present at relatively high levels in small tumors and at lower levels in larger tumors (Fig. 1*A*). In analysis of MC-38 and MCA-205 tumors, sIL-15 complexes are also produced during early tumor growth, demonstrating that production of sIL-15 complexes in tumors is not unique to B16 tumors (*SI Appendix*, Fig. S1 *A* and *B*). Similar levels of sIL-15 complexes were found in B16-ovalbumin (OVA) tumors as B16-F10 tumors (*SI Appendix*, Fig. S1*C*). As such, the B16-OVA line was used for in vivo experiments from here on as it allows the analysis of tumor-specific CD8 T cell responses. We also examined the levels of sIL-15 complexes in B16 tumors at different times postimplantation and found that sIL-15 complexes are higher at earlier stages of tumor growth and their levels are reduced with tumor growth (Fig. 1*B*). Additionally, in both B16 and MC-38 tumors, the higher levels of sIL-15 complexes occur in the earliest tumors before the infiltration of CD8 T cells and decline thereafter before the decline in numbers of CD8 TILs that occurs with tumor growth (Fig. 1*C* and *SI Appendix*, Fig. S2*A*). These findings suggest IL-15 regulates CD8 T cell numbers in the TME.

To directly examine the role of IL-15 in regulating TIL numbers, established palpable B16 tumors in WT mice were treated intratumorally with neutralizing IL-15 Ab or control Ig. Blocking IL-15 activity in the tumor led to a significant decrease in the total number of CD8 T cells and NK cells in the tumors ($P < 0.001$) but did not significantly affect the total numbers of CD4 T cells (Fig. 1*D*). To determine if endogenous IL-15 regulates proliferation of TILs, K_i-67 expression was examined in TILs in B16 tumors of mice treated with neutralizing IL-15 Ab. K_i-67 expression in CD8 and CD4 TILs was similar with IL-15 neutralization and control Ig treatment (*SI Appendix*, Fig. S2*B*), suggesting IL-15 regulates TIL numbers independent of proliferation, possibly by promoting survival and/or infiltration. TILs were also examined phenotypically and found to have similar levels of $Tim\text{-}3^+$ and $PD\text{-}1^+Tim3^+$ among both groups (*SI Appendix*, Fig. S2*C*). Decreases in TIL numbers were also observed with IL-15 blockade of MC-38 tumors (*SI Appendix*, Fig. S2*D*). Surprisingly, IL-15 blockade did not affect B16 or MC-38 tumor growth (*SI Appendix*, Fig. S2 *E* and *F*), suggesting the amount of IL-15 present in the TME is sufficient to regulate TILs but is not sufficient by itself to break tolerance against the tumor and drive tumor regression.

Since IFN-Is expressed in the TME are important for spontaneous antitumor responses (31) and we have previously demonstrated IFN-Is are potent inducers of sIL-15 complexes in vivo (17), we asked if IFN-I signaling is important for the production of sIL-15 complexes in the TME. In B16 tumors transplanted into $IFNAR^{-/-}$ mice, sIL-15 complexes were decreased in the early tumors compared with those in WT mice (Fig. 1*E*), indicating IFN-Is are important for production of sIL-15 complexes in the TME. Since IFN-Is can be induced by the STING pathway, we asked if the STING pathway was important for endogenous production of sIL-15 complexes. B16 tumors implanted into $TMEM173^{-/-}$ mice showed similar levels of sIL-15 complexes as WT mice (Fig. 1*F*), suggesting this IFN-I response was not dependent on the STING pathway. Furthermore, total numbers of CD8 T cells, CD4 T cells, and NK cells among TILs were decreased in B16 tumors implanted into $IFNAR^{-/-}$ mice compared with WT mice (Fig. 1*G*). The increase in the CD4:CD8 T cell ratio in tumors of $IFNAR^{-/-}$ mice reflects the more dramatic loss in CD8 T cells, which is consistent with the loss of IL-15 as IL-15 preferentially stimulates CD8 T cells over CD4 T cells (32). Overall, IL-15 is expressed as IL-15 complexes in the TME in an IFN-I–dependent manner and regulates the number of CD8 and NK TILs.

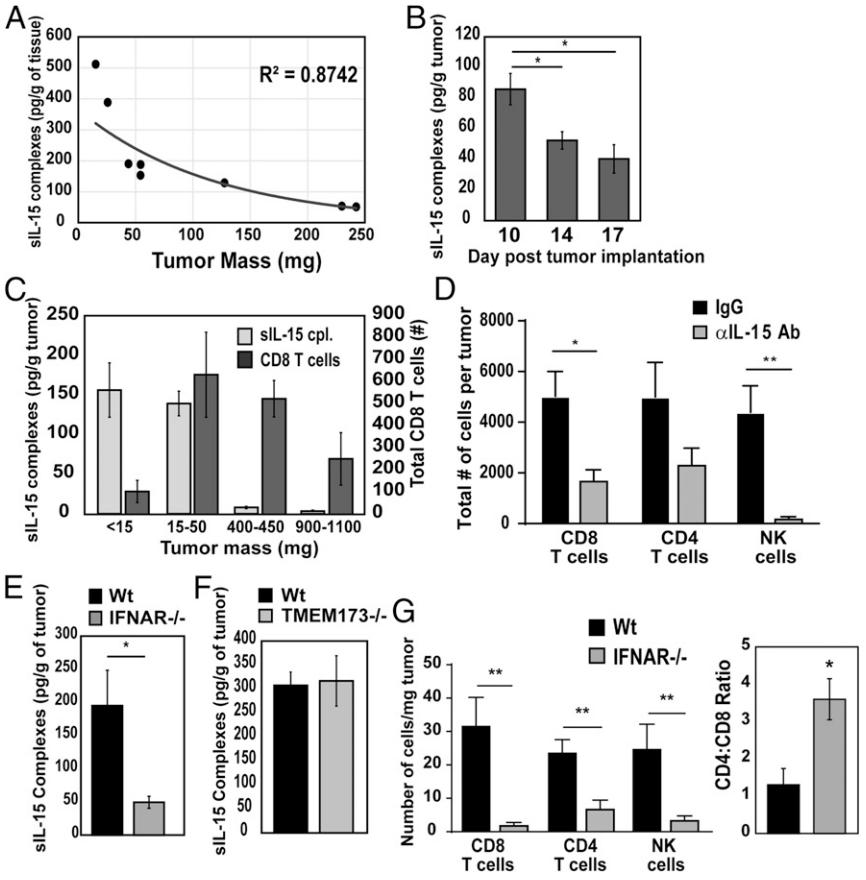

Fig. 1. sIL-15 complexes are produced in the tumor microenvironment. (*A*) B16-F10 tumor cells were injected (0.3×10^6 cells, s.c.) into WT mice. Tumors were dissociated and supernatants analyzed for sIL-15 complexes using ELISA. Levels of sIL-15 complexes in B16-F10 tumors of different masses isolated at the same time postimplantation. (*B*) Levels of sIL-15 complexes in B16-F10 tumors isolated at 10, 14, and 17 d posttumor implantation. $n = 5$ mice per group. (*C*) Levels of sIL-15 complexes (light gray bar, *Left* axis) and total CD8 T cells per tumor (dark gray bars, *Right* axis) in B16-F10 tumors grouped by tumor size. (*D*) B16-OVA tumors implanted into WT mice were treated intratumorally with αIL-15Ab (50 μg) or rat IgG 9 d after tumor implantation. Tumor lymphocytes were analyzed 3 d later by flow cytometry and total cell numbers were normalized to tumor weight. (*E*) B16-OVA cells were injected (0.3×10^6 cells, s.c.) into WT or IFNAR$^{-/-}$mice; levels of sIL-15 complexes in tissues were analyzed 10 d postimplantation; $n = 4$–8 mice per group. Tumor masses range from 10 to 55 mg [WT average (ave) = 34.7 ± 17.6, KO ave = 41.1 ± 16.6]. (*F*) Levels of sIL-15 complexes in B16-OVA tumors implanted in TMEM173$^{-/-}$ mice 9 d tumor postimplantation. $n = 5$–8 mice per group. Average tumor weights were WT 21 ± 7.1; KO = 19.8 ± 3.3. (*G*) The numbers of CD8 T cells, CD4 T cells, and NK cells in B16-OVA tumors implanted into WT or IFNAR$^{-/-}$ mice were analyzed by flow cytometry and normalized to tumor weight. One representative experiment of three performed is shown. Error bars represent SEM. $^*P < 0.05$, $^{**}P < 0.01$.

Cellular Sources of sIL-15 Complexes. To address the extent to which sIL-15 complexes were derived from the tumor stroma, levels of sIL-15 complexes were measured in tumors implanted into WT and IL-15Rα$^{-/-}$ mice. sIL-15 complexes were not detected in B16 tumors implanted into IL-15Rα$^{-/-}$ mice (Fig. 2*A*), indicating the sIL-15 complexes were derived from the tumor stroma and not the tumor cells. However, when either MC-38 colon carcinoma or MCA-205 fibrosarcoma tumor cells were implanted in IL-15Rα$^{-/-}$ mice, sIL-15 complexes in the interstitial fluid of these tumors were still abundant, suggesting the tumor cells themselves were producing sIL-15 complexes (Fig. 2*B*). This was confirmed in analysis of culture supernatants obtained from these tumor cell lines (Fig. 2*C*). Tumor cell lines, such as BP-1 melanoma cells, MB49 bladder carcinoma, and 4T1 mammary tumor cells also produced sIL-15 complexes while T3M4 pancreatic cancer, A20 lymphoma, and CT26 colon carcinomas cell lines did not produce detectable levels of sIL-15 complexes (*SI Appendix*, Fig. S3). Thus, the ability of tumor cell lines to produce sIL-15 complexes is variable, but is not necessarily dictated by the tissue of origin. Therefore, we have identified different scenarios of sIL-15 complex production: one where sIL-15 complexes are exclusively derived from the TME (i.e., B16) and the other where sIL-15 complexes can come from both the tumor and the tumor stroma (i.e., MCA-205, MC-38).

Since we demonstrated that sIL-15 complexes present in the B16 tumors are derived exclusively from the tumor stroma, we chose to use the B16 model to further investigate the nontumor-derived sources of sIL-15 complexes in the TME. We utilized various IL-15Rα conditional knockout mouse models: IL-15Rα floxed mice (IL-15Rα$^{fl/fl}$) crossed to CD11c-Cre Tg mice or LysM-Cre Tg mice to delete IL-15Rα primarily in DCs and phagocytic cells (macrophage and neutrophils), respectively, as previously described (14). Loss of IL-15 expression from either DCs (Fig. 2*D*) or phagocytic cells (Fig. 2*E*) led to a significant reduction in the levels of sIL-15 complexes in B16 tumors, suggesting both cell types are contributing to baseline sIL-15 complex levels in the TME. To examine the contribution of monocytes, B16 cells were implanted into CCR2-DTR Tg$^+$ and Tg$^-$ littermates and treated with diphtheria toxin (DT) (200 ng, i.p. every 2 d) to deplete CCR2$^+$ myeloid cells. Treatment with DT consistently decreased the levels of sIL-15 complexes in B16 tumors implanted into DTR-Tg$^+$ mice compared with the tumors in DT-treated Tg$^-$ mice (Fig. 2*F*); however, these differences did not reach statistical significance ($P < 0.1$). To examine the specific contribution from tumor-associated neutrophils or granulocytic myeloid-derived suppressive cells (MDSCs), sIL-15 complexes were analyzed in tumors from mice treated with Ly6G-depleting Ab. This treatment had no effect on levels of sIL-15 complexes, suggesting neutrophils/MDSCs are not a significant source of sIL-15 complexes in the TME (Fig. 2*G*). In no model examined, were sIL-15 complexes reduced by more than 50%, indicating that there are multiple myeloid sources of sIL-15 complexes in the TME, including CD11c$^+$, LysM$^+$ phagocytic cells, and monocytic cells.

We also examined the contribution of nonhematopoietic cells as sources of sIL-15 complexes using bone marrow (BM) chimeras. IL-15Rα$^{-/-}$ BM chimeras (Rko BM → WT recipients) and WT control BM chimeras (WT BM → WT recipients) were generated, and reconstitution of the hematopoietic compartment was confirmed ~12 wk later followed by s.c. implantation of B16 tumor cells. Tumors and spleens were analyzed for sIL-15 complexes 2 wk later. B16 tumors isolated from IL-15Rα$^{-/-}$ BM chimeras expressed lower levels of sIL-15 complexes than WT BM chimeras ($P < 0.1$) (Fig. 2*H*), indicating nonhematopoietic cells may be an additional source of sIL-15 complexes in the TME. Overall, our analyses demonstrate that there are multiple sources of sIL-15 complexes in the TME, including multiple myeloid cells,

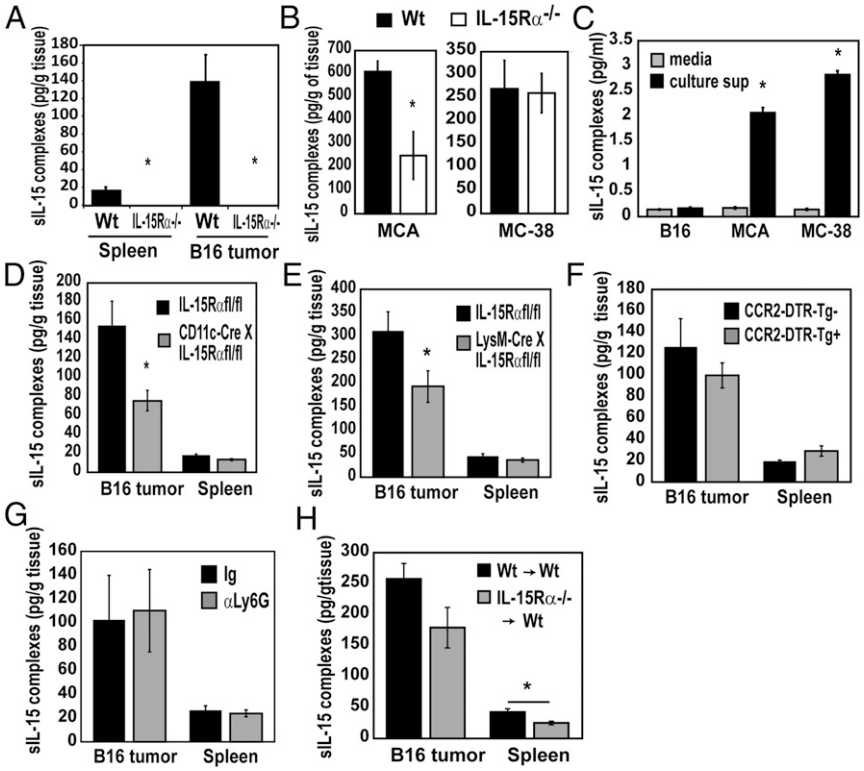

Fig. 2. Cellular sources of sIL-15 complexes in the tumor microenvironment. Tumor cells were injected (0.3×10^6 cells, s.c.) into WT or IL-15Rα$^{-/-}$ mice. Tumors and spleens were dissociated and supernatants were analyzed for sIL-15 complexes using ELISA. (*A*) Levels of sIL-15 complexes in B16-OVA tumors implanted in WT and IL-15Rα$^{-/-}$ mice; $n = 2$–3 mice per group. Error bars represent SD. (*B*) Levels of sIL-15 complexes in MCA-205 tumors (day 9–11) and MC-38 tumors (day between 9 and 14) isolated from WT and IL-15Rα$^{-/-}$ mice. Average tumor mass (mg) of MCA-205 tumors were WT = 21.6 ± 17, Rko = 24.8 ± 6; average tumor mass of MC-38 tumors WT = 32.8 ± 8.3, Rko = 28.4 ± 9.7. (*C*) Levels of sIL-15 complexes present in tumor cell culture supernatants. Error bars represent SEM. (*D* and *E*) Levels of sIL-15 complexes in spleens and B16-OVA tumors isolated from control IL-15Rα$^{fl/fl}$ (black), CD11c-Cre$^{+/+}$ × IL-15Rα$^{fl/fl}$ (gray), and LysM-Cre$^{+/+}$ × IL-15Rα$^{fl/fl}$ (gray) mice 10 d tumor postimplantation ($n = 3$–5 mice per group), one representative experiment of three is shown. (*F*) B16-OVA tumors were implanted in CCR2-DTR-Tg^{-} and CCR2-DTR-Tg^{+} mice. Beginning 7 d postimplantation, mice were treated i.p. with either PBS or DT every 2 d. Tumors and spleens were isolated 12–13 d postimplantation. Tumors ranging between 50 and 100 mg were analyzed and average tumor mass was not significantly different between groups ($n = 3$ tumors per group, $n = 4$–6 spleens per group). (*G*) B16-OVA tumors were implanted in WT mice. When tumors became palpable (day 8–9), mice were treated either with αLy6G Ab (clone 1A8, 400 μg, i.p.) or rat IgG and 3 d later with αLy6G Ab (100 μg, i.p. plus 50 μg i.t.). Levels of sIL-15 complexes in B16 tumors and spleens were analyzed 2–3 d later. $n = 5$ mice per group. (*H*) Levels of sIL-15 complexes in B16-OVA tumors and spleens isolated from IL-15Rα$^{-/-}$ BM chimeras (Rko BM → WT recipients) and WT control BM chimeras (WT BM → WT recipients) 2 wk after implantation, $n = 4$–5 mice per group. Error bars represent SEM. *$P < 0.05$.

nonhematopoietic cells, and in some instances the tumor cells themselves.

The Tumor Microenvironment Is Abundant in IL-15–Expressing Myeloid Cells, Composed Predominately of CD11b^{+}Ly6C^{hi}Ly6G^{-} Cells. Our next objective was to more specifically identify the cells expressing IL-15 within the TME and determine how IL-15 expression in the TME differs from that in the spleen. To address this, B16 tumor cells were implanted into WT, IL-15 transcriptional reporter, or IL-15 translational reporter mice, allowed to grow, and tissues were isolated for flow cytometric analysis of GFP^{+} cells. Between 12 and 18 d postimplantation, GFP expression was compared in dissociated tumors and splenocytes. Among splenocytes, the majority of TCRαβ CD19 NK1.1 (lineage)$^{-}$ cells are GFP^{+} (~75%) and consist of CD11c^{hi} DCs, neutrophils (CD11b^{+}Ly6G^{+}), monocytes (CD11b^{+}Ly6C^{hi}), and macrophages (CD11b^{+}Ly6C$^{-/lo}$Ly6G^{-}), similar to that described in previous studies (28) (Fig. 3*A*). Similar to spleen, most myeloid cells in the tumor are GFP^{+} (80–90%); however, the composition of the GFP^{+} cells was different from that in the spleen. In B16 tumors, a larger portion of CD45^{+} lineage^{-} cells were CD11b^{hi}CD11c$^{lo/int}$ than in the spleen (Fig. 3*A*). Additionally, while GFP^{+} CD11c^{hi} cells and other CD11b^{lo} cells are found in the spleen, the proportion of CD11c^{hi} cells among GFP^{+} populations in the tumor are low in comparison with that observed in the spleen (Fig. 3*A*). Among the GFP^{+}CD11b^{+} cells in B16 tumors, there are three main populations: Ly6C^{hi}Ly6G^{-} (monocytic), Ly6C^{+}Ly6G^{+} (neutrophils or granulocytic MDSC), and Ly6C$^{-/lo}$Ly6G^{-} cells (Fig. 3*A*). Unlike the spleen, the GFP^{+}CD11b^{+} cells in B16 tumors were composed predominantly of Ly6C^{hi} Ly6G^{-} cells while Ly6C^{+}Ly6G^{+} cells were minimally represented (Fig. 3*A*). Similar analyses were also conducted with the MC-38 and MCA-205 cells implanted into IL-15 reporter mice. In general, the composition of GFP^{+} cells in MCA-205 and MC-38 tumors was similar to that observed in B16 tumors, except that MC-38 tumors harbored a higher percentage of CD11c^{hi}GFP^{+} cells and slightly fewer CD11b^{+}Ly6C$^{-/lo}$Ly6G^{-} cells (Fig. 3*B* and *SI Appendix*, Fig. S4*A*). MCA-205 tumors harbored slightly more CD11b^{+}Ly6C$^{-/lo}$Ly6G^{-} cells among GFP^{+} cells compared with B16 and MC-38 tumors but this was not statistically significant (Fig. 3*B* and *SI Appendix*, Fig. S4*A*). The composition of GFP^{+} cells between the two IL-15 reporter mouse lines was equivalent (*SI Appendix*, Fig. S4*B*). Overall, across multiple implantable tumor cell lines, tumor myeloid cells expressing IL-15, composed predominantly of CD11b^{+}Ly6C^{hi}Ly6G^{-} cells are abundant in established tumors.

To further define these myeloid subsets, the expression of CCR2, which is associated with inflammatory monocytes (33), was

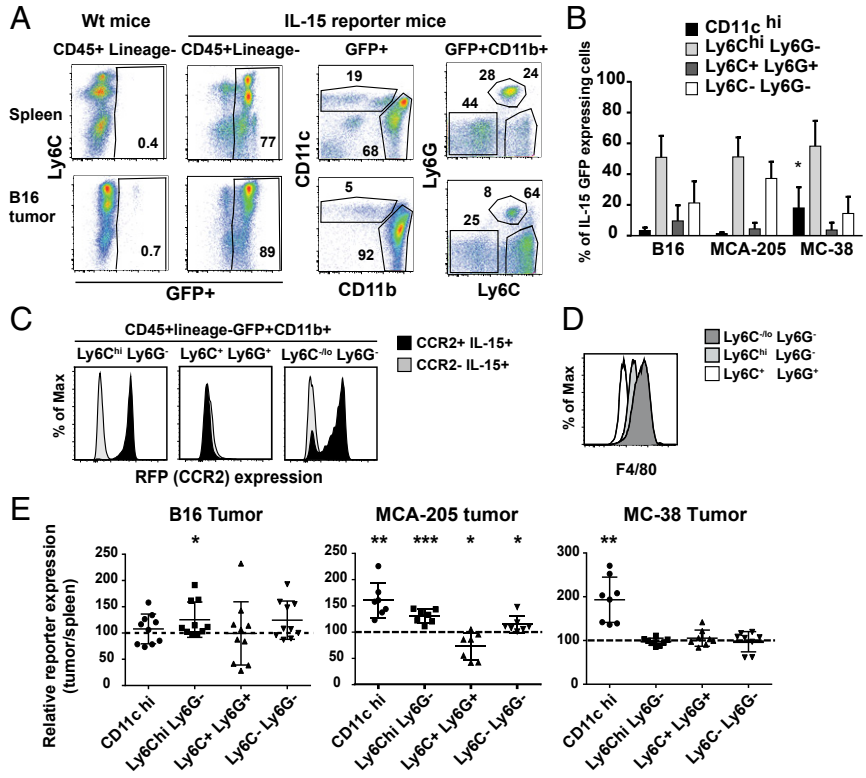

Fig. 3. CD11b^{+}CD11c$^{-/+}$Ly6C^{+} cells are the major subset expressing IL-15 in the tumor microenvironment. (*A*) Flow cytometric analysis of IL-15-GFP expressing myeloid subsets in spleens and B16-OVA tumors (200–250 mg) isolated from WT (*Left*) and IL-15 translational-GFP reporter (*Right*) mice 14 d postimplantation. Spleens and tumors from WT mice were used to set the gate for GFP^{+} cells. Expression of CD45^{+} and lineage (TCR-β, CD19, NK1.1) negative cells were used to discriminate myeloid cell populations. Myeloid cells were then gated on GFP^{+} cells and the composition of GFP^{+} cells was examined by CD11c, CD11b, Ly6G, and Ly6C expression. Representative data from one of six independent experiments are shown. (*B*) Composition of IL-15–GFP-expressing cells among CD45^{+} lineage^{-} cells present in B16-OVA, MCA-205, and MC-38 tumors isolated from IL-15 reporter mice. Tumors analyzed ranged from 35 to 100 mm^{2}. Bars show mean ± SD from $n = 7$–10 mice per group. * represents a significant difference in frequency of CD11c^{hi} cells compared with B16-OVA and MCA-205 tumors. (*C*) CCR2 reporter expression in indicated cells isolated from B16-OVA tumors implanted into either CCR2-RFP^{+}/IL-15 transcriptional GFP^{+} reporter or CCR2-RFP^{-}/IL-15–transcriptional GFP^{+} reporter. (*D*) F4/80 expression on indicated populations after gating on GFP^{+}CD11b^{+} cells in B16 tumors isolated from IL-15–transcriptional GFP reporter mice. (*E*) The relative IL-15–GFP reporter expression levels among analogous cells in spleen and tumors. GFP expression by the specific CD45^{+} lineage^{-} CD11b^{+} cell populations was calculated by dividing the mean fluorescence intensity (MFI) of the indicated population isolated from the tumor over the MFI of the analogous population from the spleen of the same mouse ($n = 7$–10 mice per group, error bars represent SEM). *$P < 0.05$, **$P < 0.01$, ***$P < 0.001$.

examined in myeloid cells in B16 tumors implanted into translational IL-15–GFP/CCR2-RFP double reporter mice. Among the GFP^{+}CD11b^{+} cells in the tumors, the Ly6C^{hi}Ly6G^{-} cells expressed high levels of CCR2 reporter, the Ly6C$^{-/lo}$Ly6G^{-}cells were predominantly CCR2^{+}, while the Ly6C^{+}Ly6G^{+} cells were uniformly CCR2^{-} (Fig. 3*C*). In addition, we examined F4/80 expression by the GFP^{+}CD11b^{+} populations in tumors and found that the Ly6C$^{-/lo}$Ly6G^{-} cells expressed higher levels of F4/80 than the other CD11b^{+} subsets, implicating these cells as part of the macrophage lineage (Fig. 3*D* and *SI Appendix*, Fig. S5). Unlike in the spleen where macrophages are F4/80^{hi}CD11b^{int} cells, an analogous population was not observed in the TME but instead, an F4/80^{lo}CD11b^{hi} population was observed (*SI Appendix*, Fig. S5).

To address whether the IL-15 expression is different in specific myeloid cells in tumors compared with the spleen, we gated on specific myeloid populations and compared the GFP expression between the spleen and the tumor within the same mice. In the B16 tumors, GFP expression was increased in the CD11b^{+}Ly6C^{hi} Ly6G^{-} compared with the spleen (Fig. 3*E*). GFP expression by CD11c^{hi} cells, CD11b^{+}Ly6C^{hi}Ly6G^{-}, and Ly6C$^{-/lo}$Ly6G^{-} cells was also increased in MCA-205 tumors compared with spleen but decreased in the Ly6C^{+}Ly6G^{+} population (Fig. 3*E*). In contrast, in MC-38 tumors, only the CD11c^{hi} cells showed increased GFP expression relative to that in the spleen (Fig. 3*E*). Overall, these findings indicate that IL-15 expression is altered among myeloid cells within the TME, depending on the myeloid cell expressing IL-15 and the tumor type.

Since IL-15Rα is required for expression of cell surface IL-15 complexes and soluble IL-15 complexes (10, 15), cell surface IL-15Rα expression by tumor myeloid cells was examined. All myeloid cell subsets expressed surface IL-15Rα with the CD11b^{+}Ly6C^{hi} cells expressing the highest levels (*SI Appendix*, Fig. S6*A*). In analysis of IL-15Rα at different stages of tumor growth, levels of IL-15Rα by the three major myeloid subsets did not significantly change between day 9 and day 14 tumors (*SI Appendix*, Fig. S6*B*). These data suggest that tumor myeloid cells are capable of both trans-presenting IL-15 and producing sIL-15 complexes.

IL-15 Expression Can Be Up-Regulated in Tumors by Activating the STING Pathway. Although IL-15 reporter^{+} cells are numerous in established tumors (Fig. 3*A*), production of sIL-15 complexes is significantly reduced in the latter (Fig. 1*A*). Therefore, we sought to determine if administrating exogenous STING agonists was capable of up-regulating production of sIL-15 complexes in the TME. Despite STING signaling not being involved in regulation of sIL-15 complexes in early tumor development, intratumoral (i.t.) injection of the STING agonist, c-di-GMP (25 μg) in large tumors (range 170–260 mg) led to an impressive up-regulation of sIL-15 complexes in the tumor (Fig. 4*A*). Importantly, these data demonstrate the IL-15–expressing cells present in the TME are

capable of producing sIL-15 complexes in the tumor at this later stage of development. To address which cell types respond to STING activation by increasing IL-15 expression, B16 tumors established in IL-15 translational reporter mice were treated i.t. with c-di-GMP, and GFP expression by myeloid cells in the tumor was examined 24 h later. In response to STING pathway activation in the TME, we observed significant increases in GFP expression on the $CD11c^{hi}$, $CD11b^{+}Ly6C^{hi}$, and $CD11b^{+}Ly6C^{-/lo}Ly6G^{-}$ tumor-infiltrating myeloid cell subsets compared with PBS treatment (Fig. 4 *B* and *C*). We also wanted to address whether stimulation of the STING pathway is capable of up-regulating sIL-15 complexes directly in tumor cells. Hence, B16, MCA-205, and MC-38 tumor cells were treated with STING agonist in vitro. As shown earlier, sIL-15 complexes were not produced by either B16-OVA or B16-F10 tumor cells, even after treatment with STING agonists (Fig. 4*D*). In contrast, STING activation did increase production of sIL-15 complexes in the tumor cell lines with baseline detectable sIL-15 complexes, including MCA-205 and MC-38 cells (Fig. 4*D*), indicating that in these tumor models, both myeloid cells and tumor cells are capable of responding to STING agonists. These results demonstrate that intratumoral activation of the STING pathway up-regulates the translation of IL-15 and the production of sIL-15 complexes in tumors, even at later stages of tumor development.

Up-Regulation of IL-15 in the Tumor Enhances CD8 T Cell Responses and Promotes Antitumor Responses. STING agonists have been shown to enhance antitumor responses when given intratumorally (34–37). As such, we asked whether tumor-specific CD8 T cell responses were increased by the STING agonist treatment. To examine this, naïve OVA-specific TCR transgenic T cells (OT-I) were CFSE labeled and injected into mice bearing B16-OVA tumors, followed by i.t. treatment with STING agonist. The frequency of OT-I T cells in tumor-draining lymph node (dLN) and spleens was increased in mice treated with c-di-GMP (Fig. 5*A*). Additionally, these OT-I T cells divided more (Fig. 5*A*). However, when similar experiments were performed to analyze OT-I T cell responses to STING agonists in WT mice treated with αIL-15 Ab, the extent of OT-I proliferation was similar (*SI Appendix*, Fig. S7 *A* and *B*), suggesting IL-15 was not critical for STING-enhanced proliferation of OT-I T cells. This was surprising considering our previous studies showed STING-mediated bystander proliferation of memory CD8 T cells was IL-15 dependent (18). Nonetheless, we found that i.t. treatment with STING agonists increased the percentage of K_i-67^{+} CD8 T cells in the dLN and the spleen but not in the tumor where frequency of K_i-67^{+} cells was already high (Fig. 5*B*). STING agonists also increased K_i-67^{+} NK cells in the spleen, while STING agonist had only a minor effect on K_i-67^{+} CD4 T cells in spleen, but not in dLN or tumor (Fig. 5*B*). Furthermore, the increase in the frequency of K_i-67 among CD8 T cells was abrogated with treatment with neutralizing IL-15 Ab (Fig. 5*B*). K_i-67 expression by NK cells with IL-15 Ab treatment is difficult to analyze as this antibody treatment leads to the disappearance of NK cells (*SI Appendix*, Fig. S7*C*) (38). The effects of i.t. STING agonist treatment on CD8 T cell effector functions were also investigated. Similar to K_i-67 expression, IFN-γ and granzyme B expression by CD8 T cells were already high in untreated tumors and treatment with c-di-GMP did not further increase this (Fig. 5*C* and *SI Appendix*, Fig. S7 *D* and *E*). However, i.t. c-di-GMP led to an increase in IFN-γ expression by CD8 T cells in the spleen that was abrogated by blocking IL-15 (Fig. 5*C*). A similar effect on IFN-γ expression by CD8 T cells was observed in dLN but was not statistically significant (Fig. 5*C*). Altogether, STING activation in the TME leads to increased proliferation of CD8 T cells and NK cells and an increased frequency of IFN-γ^{+} CD8 T cells in secondary lymphoid tissues in an IL-15–dependent manner.

We next asked whether IL-15 expression induced by STING stimulation was important for STING-mediated antitumor responses. WT and IL-15Rα$^{-/-}$ mice bearing palpable B16 tumors were treated i.t. with STING agonist and tumor growth was measured over time. In the absence of STING stimulation, tumor growth progressed faster in IL-15Rα$^{-/-}$ mice than in WT mice, providing evidence that IL-15 expression impacts baseline antitumor responses (Fig. 5 *D* and *F*). While STING agonist induced potent antitumor immunity and tumor regression in WT mice, it failed to induce tumor regression in IL-15Rα$^{-/-}$ mice (Fig. 5*D*). These results indicate that IL-15 is a critical mediator driving STING-induced tumor regression. A similar dependence on IL-15 was also observed with STING agonist treatment of MCA-205 tumors in WT and IL-15Rα$^{-/-}$ mice (*SI Appendix*, Fig. S8). Since IL-15Rα$^{-/-}$ mice have inherent deficiencies in NK cells and CD8 T cells (39), we used an IL-15 neutralizing Ab to block IL-15 in tumor-bearing WT mice treated with i.t. STING agonists (Fig. 5*E*). In the presence of IL-15 neutralizing Ab, STING-mediated tumor regression was impaired, therefore recapitulating the

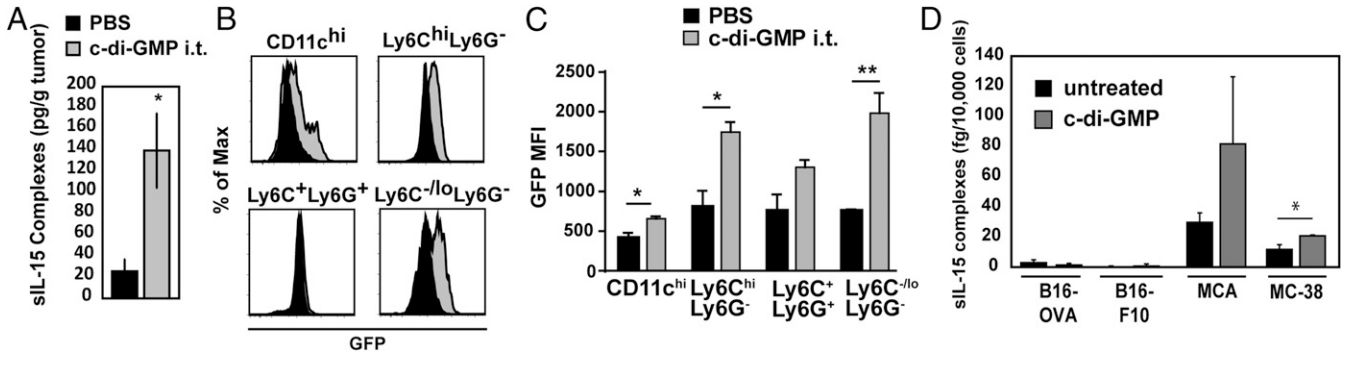

Fig. 4. Stimulation of the STING pathway up-regulates sIL-15 complexes in tumors. (*A*) STING agonist, c-di-GMP (25 μg) or PBS was injected i.t. into large, well-established B16-OVA tumors and levels of sIL-15 complexes within tumors were analyzed 1 d later. Average tumor mass was 259 mg ± 53 and 173 mg ± 59 in untreated and c-di-GMP–treated tumors, respectively. (*B*) IL-15 reporter expression in B16-OVA tumors 24 h after i.t. 2′3′-cGAMP (25 μg) or PBS. Histograms show the GFP levels on indicated cell populations in B16-OVA tumors treated with i.t. 2′3′-c-GAMP (gray histogram) or PBS (black histogram) after gating on $CD45^{+}$ $lineage^{-}CD11b^{+}$ cells. Tumors were treated 14 d after implantation into IL-15 translational reporter mice. (*C*) Graphs represent the averaged GFP levels of the respective $CD11b^{+}$ populations isolated from 2′3′-c-GAMP or PBS-treated tumors in IL-15 translational reporter mice. $n = 3$ mice per group. (*D*) Subconfluent B16-OVA, B16-F10, MCA-205, and MC-38 cells were either left untreated or treated with c-di-GMP (6.6 μg/mL) and 48 h later, culture supernatants were analyzed for levels of sIL-15 complexes and normalized to the number of cells recovered. ($n = 3$ wells per group, error bars represent SEM). *$P < 0.05$, **$P < 0.01$.

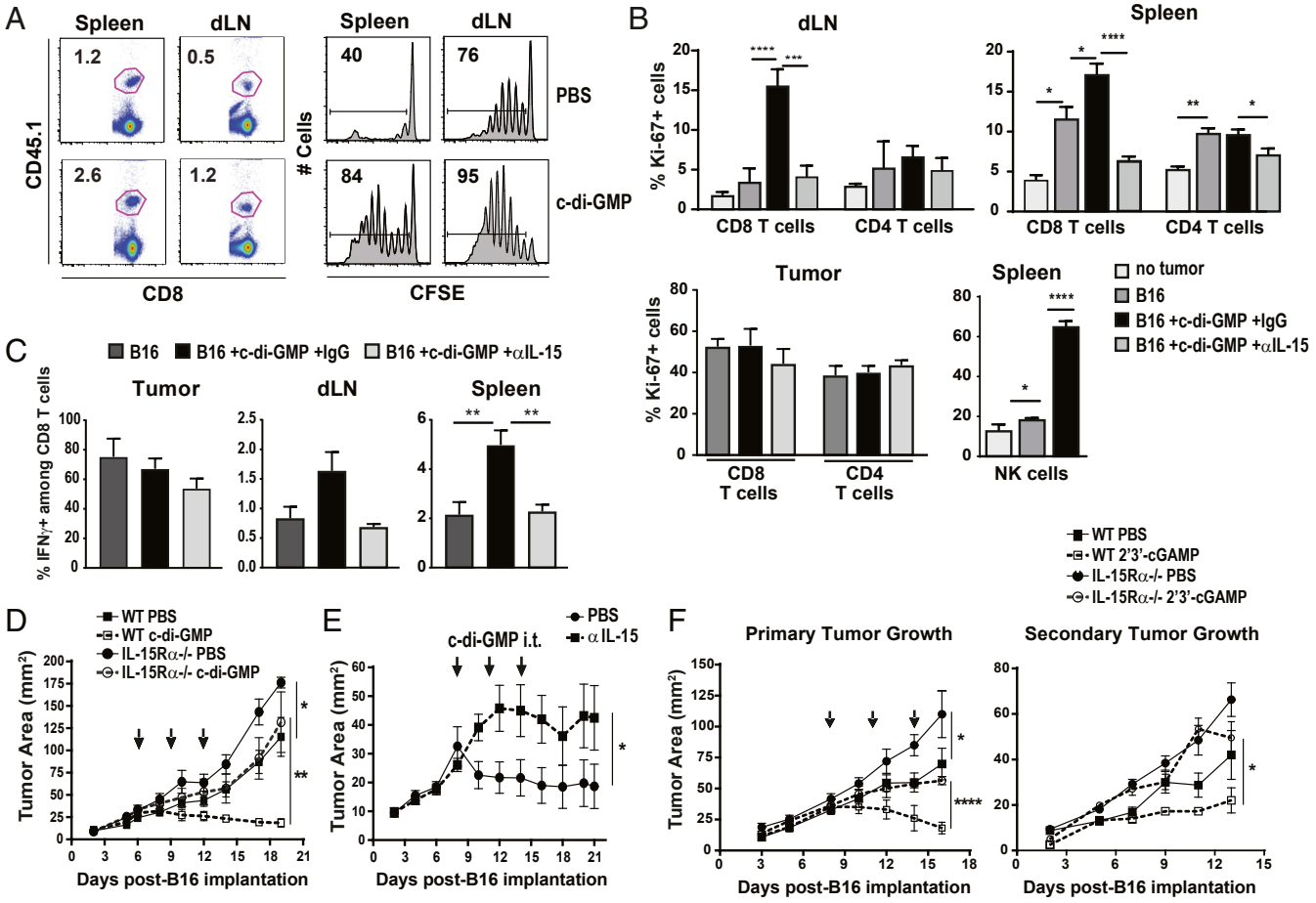

Fig. 5. STING activation in the tumor microenvironment promotes tumor regression via IL-15–dependent mechanisms. (*A*) Flow cytometry analysis of CFSE dilution in tumor-specific T cells. WT mice bearing B16-OVA tumors were injected with 0.5×10^6 CFSE-labeled OT-I cells on day 7 postimplantation, and received one i.t. treatment with c-di-GMP (25 μg) once tumors became palpable. Three days posttreatment, the mice were killed and spleen and draining lymph nodes were analyzed by flow cytometry. (*B*) B16-OVA tumors were implanted into WT mice and treated with c-di-GMP on day 12 postimplantation. IL-15 Ab (50 μg) was delivered i.p. 1 d before and on the same day as treatment with c-di-GMP. dLNs, spleens, and tumors were isolated 3 d later and K_i-67 staining by CD8 T cells, CD4 T cells, and NK cells was measured by flow cytometry. (*C*) Graphs show average frequency of IFN-γ^+ cells among CD8 T cells isolated from B16 tumors, dLNs, and spleens in similar experiment as shown in Fig. 5B. (*D*) B16-OVA tumor growth in WT and IL-15R$\alpha^{-/-}$ mice treated with i.t. injections of c-di-GMP (25 μg) or PBS on days 7, 10, and 13 postimplantation (indicated by arrows). (*E*) Tumor growth of B16-OVA tumors in WT mice treated systemically with neutralizing IL-15 Ab or PBS (7 d posttumor implantation) followed by three i.t. treatments with c-di-GMP (25 μg). Tumor growth was significantly different between groups at days 9–15 and days 20–21, $P < 0.05$. (*F*) WT and IL-15R$\alpha^{-/-}$ mice bearing B16-OVA tumors on the right flank were implanted with a secondary B16-OVA tumor on the left flank 72 h later. The primary tumors were treated with three i.t. injections of 2′3′-cGAMP (15 μg) or PBS on days 7, 10, and 13. *Right* shows tumor growth of primary tumors while *Left* shows tumor growth of secondary tumors ($n = 5$ per group, error bars represent SEM). $^*P < 0.05$, $^{**}P < 0.01$, $^{***}P < 0.001$, $^{****}P < 0.0001$.

results observed in IL-15R$\alpha^{-/-}$ mice. Since we observed that IL-15 reporter expression increased upon treatment with STING agonist, we asked whether the expression of IL-15 by CD11c$^+$ cells was important for STING-mediated tumor regression. To this end, B16 tumors were implanted into both CD11c-Cre Tg X IL-15R$\alpha^{fl/fl}$ mice followed by intratumoral treatment with c-di-GMP or PBS. The ability of STING agonist treatment to induce regression of tumors was not impaired in CD11c-Cre Tg X IL-15R$\alpha^{fl/fl}$ mice (*SI Appendix*, Fig. S9), suggesting the tumor regression was not dependent on up-regulation of IL-15 by CD11c$^+$ cells in response to STING stimulation. Additionally, tumor growth was not increased in untreated CD11c-Cre Tg X IL-15R$\alpha^{fl/fl}$ mice (*SI Appendix*, Fig. S9).

Since STING agonists have been shown to induce potent systemic antitumor responses resulting in regression of distant tumors (36, 37), we investigated whether this abscopal effect of STING agonist against a secondary tumor required the cooperation of IL-15 (Fig. 5*F*). We also examined whether tumor regression could be induced by other STING agonists, such as 2′3′c-GAMP that represents a type of STING agonist produced by mammalian cells. We found intratumoral 2′3′c-GAMP induced tumor regression similar to c-di-GMP in an IL-15–dependent manner (Fig. 5*F*). Furthermore, STING-mediated tumor regression of a secondary tumor was also dependent on IL-15. These results show the important role of the IL-15 produced in the TME in endogenous and STING-agonist induced antitumor immunity.

Discussion

There is abundant evidence that IL-15 and its agonists through their ability to target enhanced responses of cytolytic T cells and NK cells, are promising agents for cancer therapy when used systemically. While therapeutic approaches use superphysiological doses of IL-15, IL-15 is a cytokine that is constitutively expressed in multiple tissues by many cell types to maintain the normal homeostasis of T cells and NK cells. Nonetheless, increased IL-15 expression is observed after innate immune cell activation and transiently stimulates cytolytic lymphocyte responses (18, 40).

Hence, IL-15 can also act as a proinflammatory factor. With these antitumor and proinflammatory properties, we asked how the expression of IL-15 is regulated in the immunosuppressive TME. This is significant as recent studies have provided evidence that IL-15 expression within tumors correlates to better clinical and antitumor responses (8, 41). These studies suggest that in addition to its systemic actions, IL-15 can promote antitumor functions within the TME. Our study described here demonstrates that IL-15 is not only present in the TME but is subjected to dynamic regulation capable of enhancing antitumor responses.

By using IL-15 GFP reporter mice, we specifically identify the cell types that express IL-15 at the transcriptional and translational level in the TME. Because IL-15 can be regulated at the posttranscriptional level (42), the IL-15 translational reporter line was expected to better report IL-15 expression than the IL-15 transcriptional reporter line. However, we did not observe notable differences in the cell types expressing IL-15 in tumors between the two reporter lines, suggesting that the translation and transcription of IL-15 are coordinated within the TME. We did see differences in the composition of cells expressing IL-15 in tumors compared with the spleen. In general, the cell types expressing IL-15 in tumors were more limited in nature than those in spleens, consisting mainly of three myeloid populations: a monocytic subset, a granulocytic subset, and a macrophage subset. The precise nature of these cells is not clear as tumor myeloid cells are plastic and subjected to influences from the microenvironment (43). The most abundant cells expressing IL-15 in tumors, the $CD11b^{+}Ly6C^{hi}Ly6G^{-}$ cells have a phenotype consistent with inflammatory monocytes. These $CD11b^{+}Ly6C^{hi}$ cells could represent recently infiltrated monocytes or monocytic MDSC-like cells, or a mixture of both. Likewise, $CD11b^{+}Ly6G^{+}$ cells could consist of either tumor-associated neutrophils and/or granulocytic MDSCs. While the true nature of these $Ly6C^{hi}$ and $Ly6G^{+}$ cells in the tumor is uncertain, their mere expression of IL-15, a factor that stimulates cytolytic cells is more consistent with conventional, inflammatory counterparts (monocyte and neutrophil) rather than an immune-suppressive subset (i.e., MDSC). Moreover, the level of GFP expression of $Ly6C^{hi}$ cells, $Ly6G^{+}$ cells, and $Ly6C^{-/lo}Ly6G^{-}$ cells in the B16 and MC-38 tumors was largely similar or slightly increased compared with the analogous cells in the spleen, which represent the conventional IL-15 expressing cell types (i.e., monocyte, neutrophils, and macrophages). Interestingly, IL-15 expression by $CD11c^{hi}$ cells was increased in MCA-205 and MC-38 tumors compared with spleens, which could be indicative of an inflammatory response by tumor DCs. Conversely, we observed decreases in IL-15 GFP levels in $CD11b^{+}Ly6G^{+}$ cells in MCA-205 tumors compared with the spleen, suggesting that either signals in the TME of MCA-205 tumors are down-modulating IL-15 in tumor-associated neutrophils or IL-15 expression decreases as cells differentiate into granulocytic MDSCs. Overall, in these analyses we see evidence that TME induces specific changes in IL-15 expression on particular subsets of myeloid cells, which can vary depending on tumor type.

While these reporter systems report the expression of IL-15 mRNA and protein, there are additional layers of IL-15 expression, such as cell surface IL-15/IL-15Rα and its cleavage into sIL-15 complexes that these models are not able to detect. Cell surface IL-15 in tumor myeloid cells was undetectable, similar to our previous studies examining lymphoid tissues during the steady state (13). Nonetheless, sIL-15 complexes in tumors are abundant in early tumors and at decreased levels in larger tumors. This high level of sIL-15 complexes is due in part to the low tumor:stromal cell ratio and thus it is not surprising that the relative level of sIL-15 complexes decrease as tumors grow since the tumor:stromal cell ratio increases. However, we demonstrate that IFN-Is contributed to early production of sIL-15 complexes, indicating that inflammatory signals as well as tumor:stroma ratio together dictate levels of sIL-15 complexes. The increased levels of sIL-15 complexes in early tumors is consistent with the emerging paradigm that TME can produce inflammatory signals in early stages of tumor development but become more immunosuppressive as tumors grow (30). In our analysis of advanced tumors, we do not have evidence that production of sIL-15 complexes is being actively suppressed but we did demonstrate that levels of sIL-15 complexes in established tumors could be increased by activation of the STING pathway. These findings demonstrate that the IL-15-expressing cells present are capable of producing sIL-15 complexes in established tumors but may lack the inflammatory signals needed for optimal production of sIL-15 complexes. Altogether, our results suggest that IL-15, expressed as sIL-15 complexes, is a component of the inflammatory milieu in the TME.

We provide evidence that IL-15 is not only present in the TME and regulated by inflammatory signals, but more importantly, is capable of enhancing antitumor responses upon up-regulation. While we found that inhibiting IL-15 in the TME led to decreases in CD8 and NK cell TILs, this treatment did not affect tumor growth. This is somewhat surprising as multiple studies have implicated the mere presence of cytolytic TILs as a parameter dictating antitumor responses (1, 44). As such, we interpret our findings as evidence that the amount of IL-15 present in the TME is sufficient to regulate TILs but is not sufficient to break tolerance. In contrast, up-regulating IL-15 to higher levels, through activation of the STING pathway, is capable of breaking tolerance. Stimulation of the STING pathway using either STING agonists locally or in response to irradiation-induced cell death has been shown to be a potent inducer of antitumor immunity mediated by CD8 T cells leading to tumor regression and abscopal effects against distant tumors (34–37). Induction of IFN-Is is the major outcome of stimulating the STING pathway and it is well established that IFN-I induction of IL-15 is an important mechanism mediating IFN-I stimulation of CD8 T cells (32, 45). As such, our results demonstrating that STING-mediated tumor regression was dependent on IL-15 shows that stimulation of IL-15 by STING agonists is a major mechanism driving its antitumor immunity. Specifically, we observed that STING-mediated stimulation of CD8 T cells and NK cells in the secondary lymphoid tissue was IL-15 dependent. Since we did not observe this with OVA-specific T cells, we suspect the IL-15–induced response represents a broader T cell response, whereby IL-15 stimulates memory-phenotype T cells, such as that described as bystander proliferation (32) or serves as a supportive cytokine or signal 3 for T cell activation. Alternatively, IL-15 may have more dramatic effects on T cells with a lower TCR affinity, which are more representative of tumor-specific T cells. In studies examining T cell responses to sIL-15 complexes plus cognate antigen, Stoklasek et al. (46) showed the peptide plus sIL-15 complexes had synergistic effects on proliferation of low-affinity T cells while the response of high-affinity OT-I T cells to peptide plus sIL-15 complexes was increased minimally compared with the single stimulation. Additionally, there is evidence that IL-15 can enable T cells to eliminate tumors in an antigen-independent manner (41).

Our findings that sIL-15 complexes are also generated by tumor cells in MCA-205 and MC-38 tumors is a reminder that myeloid cells are not the only endogenous source of IL-15. Since IL-15 is widely expressed in normal tissues and among most cells types, we do not think the production of sIL-15 complexes by MCA-205 and MC-38 tumors is an abnormal attribute acquired with transformation. For example, intestinal epithelial cells are a major source of IL-15 in the intestines (23); therefore, it is not surprising that MC-38 colon carcinoma cells produce sIL-15 complexes. In addition, multiple studies along with our analysis of tumors in $IL\text{-}15R\alpha^{-/-}$ BM chimeras show that nonhematopoietic cells are a source of IL-15 (22, 47). Conversely, we identified tumor cell lines that do not produce sIL-15 complexes. With

these tumor cell lines, the absence of sIL-15 complexes could be a result of transformation similar to the observation by Galon and coworkers showing deletion of IL-15 in a subset of human colon carcinomas (8). The correlation of IL-15 deletion in colorectal tumors with decreased tumor-infiltrating T cells and worse clinical outcome provides evidence that total IL-15 production within a tumor dictates the antitumor response. However, in cases where IL-15 is deleted in the tumor, our findings reveal there is still the opportunity to enhance IL-15 production by the tumor stromal cells.

In conclusion, this study demonstrates that IL-15 is produced as sIL-15 complexes early after tumor establishment by cells in the TME and in some instances also by the tumor itself. With tumor growth, the relative levels of sIL-15 complexes decrease because the tumor:stroma increases. Additionally, sIL-15 com plexes may be low in established tumors because overt stimulation is absent, since our analysis of IL-15 reporter mice show that IL-15–expressing cells are still abundant. Despite the immunosuppressive milieu of the TME, these IL-15–expressing cells can up-regulate production of sIL-15 complexes upon stimulation by inflammatory signals. Remarkably, the IL-15 produced in response to local inflammatory signals is critical for mediating tumor regression and antitumor immunity. Overall, our study reveals the dynamic regulation of IL-15 in the TME and its importance in antitumor immunity. These findings provide insight into an unappreciated attribute of the tumor landscape that contributes to antitumor immunity, which can be manipulated therapeutically to enhance antitumor responses.

Experimental Procedures

Mice. C57BL/6 (WT) and CD45.1$^+$ C57BL/6 mice were purchased from National Cancer Institute/Charles River. All transgenic and gene-deficient mice used are on the C57BL/6 background. IL-15Rα$^{fl/fl}$ (14), CD11cCre (48), LysM-Cre (49), and Tmem173$^{-/-}$ mice (50) were purchased from The Jackson Laboratory. IL-15Rα$^{-/-}$ knockout (Rko) mice (39) were originally generated and obtained by Averil Ma, Department of Medicine, University of California, San Francisco, CA, through Leo Lefrancois, Department of Immunology, University of Connecticut, Farmington, CT and backcrossed to the C57BL/6 line. CCR2-DTR Tg mice (51) were generated and provided by Eric G. Pamer, Memorial Sloan Kettering Cancer Center, New York, NY. IFNAR1$^{-/-}$ mice were provided by Paul W. Dempsey, Department of Microbiology and Molecular Genetics, University of California, Los Angeles, and Tadatsugu Taniguchi, Department of Immunology, Tokyo University, Tokyo Japan, to W. Overwijk, Department of Melanoma Medical Oncology, University of Texas MD Anderson Cancer Center (UTMDACC), Houston, TX and crossed to the C57BL/6 background (52). IL-15 transcriptional reporter mice were generated by Leo Lefrancois (27). IL-15 translational reporter mice (IL-15 TE) were provided by Pippa Marrack and Ross Kedl, Integrated Department of Immunology, University of Colorado, Denver, CO (29). CCR2-RFP reporter mice (53) were originally obtained from The Jackson Laboratory through Tomasz Zal, Department of Immunology, UTMDACC and bred to the IL-15 transcriptional reporter mice to generate GFP$^+$/RFP$^+$ reporter mice. All mice described were maintained under specific pathogen-free conditions at the institutional animal facility. The animal facility is fully accredited by the Association of Assessment and Accreditation of Laboratory Animal Care International. All animal procedures were conducted on mice between 6 and 10 wk of age, in accordance with the animal care and use protocols (100409934) approved by the Institutional Animal Care and Use Committee at the UT MD Anderson Cancer Center.

To generate BM chimeras, BM was collected from the tibia and femurs of IL-15Rα$^{-/-}$ (CD45.2) and WT (CD45.2) mice and depleted of T cells as previously described (21). WT (CD45.1) recipients were irradiated with 1,000 RADs and injected i.v. with 5×10^6 BM cells. BM reconstitution was confirmed 8–12 wk later by analysis of BM-derived cells (CD45.2$^+$) in the peripheral blood before tumor implantation. Myeloid cells present in tumors isolated from BM chimeras were 95–99% CD45.2$^+$ donor BM derived (*SI Appendix*, Fig. S10 *A* and *B*).

Tumor Implantation, Treatment, and Monitoring. B16-F10 melanoma cells (B16), B16-F10 cells expressing OVA (B16-OVA), and MC-38 murine colon adenocarcinomavtumor cell lines were obtained from W. Overwijk and maintained in RPMI culture medium containing 10% FBS, 1% Hepes, 1% L-glutamine, and 1% penicillin/streptomycin (P/S). MCA-205 fibrosarcoma were obtained from Tomasz Zal, and maintained in IMDM culture medium containing 5% FBS, 1% P/S and 50 μM 2-ME. After trypsinizing and washing, 300,000 cells were injected s.c. into the flank of the indicated mice. Tumor growth was measured every other day using a caliper and tumor surface area (mm^2) was calculated as length × width. Mice were killed at various times post-implantation or when tumors reached 200 mm^2. For analysis of tumor-specific T cell responses, naïve CD45.1$^+$ OT-I TCR transgenic CD8 T cells (RAG$^{-/-}$) were isolated from LNs and spleen, labeled with 2 mM CFSE, and adoptively transferred to CD45.2$^+$ WT recipients (between $0.1–0.5 \times 10^6$ OT-I T cells per mouse).

Analysis of Cytokine Expression and Lymphocytes. For analysis of sIL-15 complexes, spleens and tumors were weighed before being homogenized in a constant volume of PBS and pelleted by centrifugation. Supernatants were collected and analyzed for levels of sIL-15/IL-15Rα complexes using an ELISA specific for murine soluble IL-15/IL-15Rα complexes (eBioscience) according to manufacturer's recommendations. The amount of sIL-15 complexes present in the respective tissue was normalized to tissue weight and expressed as the amount of sIL-15 complexes per gram of tissue.

For analysis of immune cells and IL-15 reporter expression in tumors, tumors were isolated, digested in RPMI media, 5% FCS and 100 units/mL collagenase, 1 mM $CaCl_2$ and 1 mM $MgCl_2$ for 30 min at 37 °C with stirring and then subjected to a 44–67% Percoll centrifuge gradient. Cells in the interphase were harvested, washed, and then stained for flow cytometric analysis. Spleens and LNs were homogenized in HBSS containing Hepes, L-glutamine, gentamicin, and P/S using frosted slides. RBCs were lysed with Tris-ammonium chloride. All cells were filtered through a 70-μm nitex before staining. For flow cytometric analysis, cells were stained in 1× PBS containing 0.2% BSA and 0.1% NaN_3 with appropriately diluted Ab at 4 °C for at least 20 min. K_i-67 and granzyme B staining were conducted after staining cell surface molecules and permeabilization using the FoxP3/transcription factor staining buffer set according to manufacturer's instructions (eBioscience). For IFN-γ staining, isolated lymphocytes were stimulated in the presence of plate-bound CD3Ab for 5 h in the presence of Golgiplug (BD Biosciences). IFN-γ staining was conducted after staining for cell surface molecules and permeabilization using Cytofix/Cytoperm buffer according to manufacturer's instructions (BD Biosciences). The following mAbs were purchased from BD Biosciences, eBioscience, or BioLegend: CD45, CD45.1, CD45.2, CD19, CD3, TCRβ, CD11b, CD11c, Ly6G, Ly6C, F4/80, CD8, NK1.1, CD44, K_i-67, IFN-γ, and granzyme B. Lineage$^+$ cells were identified as CD19$^+$, TCRβ$^+$, or NK1.1$^+$. Rat IgG2a-APC (BioLegend) was used as an isotype control for F4/80-APC, while rat IgG1-PE (BD Biosciences) was used as an isotype control for IFN-γ-PE and granzyme B-PE. Flow cytometric data were acquired with a LSRII (BD Biosciences) or LSR Fortessa (BD Biosciences) and analyzed with Flowjo software version 9.7.6.

Cell Depletions, STING Agonist Treatments, and IL-15 Neutralization. To deplete mice of Ly6G$^+$ cells, mice were treated i.p. with αLy6G mAb (clone 1A8, 400 μg, BioXcell) or rat IgG (Jackson ImmunoResearch Laboratories) when tumors became palpable (day 8–9) and 3 d later with αLy6G mAb (100 μg i.p. and 50 μg i.t.). To deplete CCR2$^+$ cells, CCR2-DTR Tg and WT mice were treated with 250 ng of diphtheria toxin (Sigma) every 2 d starting 4 d posttumor implantation. Efficiency in depletion of Ly6G$^+$ cells and Ly6C$^+$ monocytes in the respective models were confirmed by flow cytometry and see *SI Appendix*, Fig. S11 *A* and *B*. Levels of sIL-15 complexes in B16 tumors and spleens were analyzed 2–3 d later by ELISA as described. For stimulation of the STING pathway, mice were administered i.t. c-di-GMP or 2′3′-cGAMP (Invivogen) at the indicated doses. Neutralizing IL-15 mAb (clone M96) (38) was obtained from Amgen. For systemic neutralization of IL-15, mice received one treatment (50 μg, i.p.) of αIL-15 mAb at the indicated time after tumor implantation. Mouse IgG2a (Jackson ImmunoResearch Laboratories) was used as the isotype control. For local neutralization of IL-15, IL-15 Ab (50 μg) was delivered intratumorally when tumors become palpable. Efficient neutralization of IL-15 with antibody was confirmed by the absence of NK cells (*SI Appendix*, Fig. S7*D*).

Statistical Analysis. Statistical differences were determined by a two-tailed Student's *t* test. Analyses were performed using GraphPad Prism, version 6 (GraphPad Software) or Microsoft Excel 2010.

ACKNOWLEDGMENTS. We thank Dr. Willem Overwijk for sharing IFNAR1$^{-/-}$ mice and tumor cell lines; Dr. Eric Pamer for the CCR2-DTR Tg mice; and Drs. Lynn Puddington, Ross Kedl, and Tomasz Zal for IL-15 transcriptional reporter mice, IL-15 translational reporter mice, and CCR2-RFP reporter mice, respectively. This research was supported by NIH Predoctoral Training Grant CA009598 (to S.M.A.), a seed fund from the Center for Inflammation and Cancer at the MD Anderson Cancer Center (to K.S.S.), and First year medical student summer research program, MD Anderson Cancer Center (to G.P.) Cancer Prevention Research Institute of Texas (K.S.S.).

1. Galon J, et al. (2006) Type, density, and location of immune cells within human colorectal tumors predict clinical outcome. *Science* 313:1960–1964.
2. Kim ST, et al. (2013) Tumor-infiltrating lymphocytes, tumor characteristics, and recurrence in patients with early breast cancer. *Am J Clin Oncol* 36:224–231.
3. Piersma SJ, et al. (2007) High number of intraepithelial CD8+ tumor-infiltrating lymphocytes is associated with the absence of lymph node metastases in patients with large early-stage cervical cancer. *Cancer Res* 67:354–361.
4. Kmiecik J, et al. (2013) Elevated CD3+ and CD8+ tumor-infiltrating immune cells correlate with prolonged survival in glioblastoma patients despite integrated immunosuppressive mechanisms in the tumor microenvironment and at the systemic level. *J Neuroimmunol* 264:71–83.
5. Klebanoff CA, et al. (2004) IL-15 enhances the in vivo antitumor activity of tumor-reactive CD8+ T cells. *Proc Natl Acad Sci USA* 101:1969–1974.
6. Yu P, et al. (2012) Simultaneous inhibition of two regulatory T-cell subsets enhanced interleukin-15 efficacy in a prostate tumor model. *Proc Natl Acad Sci USA* 109: 6187–6192.
7. Yu P, Bamford RN, Waldmann TA (2014) IL-15-dependent CD8+ CD122+ T cells ameliorate experimental autoimmune encephalomyelitis by modulating IL-17 production by CD4+ T cells. *Eur J Immunol* 44:3330–3341.
8. Mlecnik B, et al. (2014) Functional network pipeline reveals genetic determinants associated with in situ lymphocyte proliferation and survival of cancer patients. *Sci Transl Med* 6:228ra37.
9. Curran MA, et al. (2013) Systemic 4-1BB activation induces a novel T cell phenotype driven by high expression of Eomesodermin. *J Exp Med* 210:743–755.
10. Dubois S, Mariner J, Waldmann TA, Tagaya Y (2002) IL-15Ralpha recycles and presents IL-15 in trans to neighboring cells. *Immunity* 17:537–547.
11. Bergamaschi C, et al. (2008) Intracellular interaction of interleukin-15 with its receptor alpha during production leads to mutual stabilization and increased bioactivity. *J Biol Chem* 283:4189–4199.
12. Schluns KS, Klonowski KD, Lefrançois L (2004) Transregulation of memory CD8 T-cell proliferation by IL-15Ralpha+ bone marrow-derived cells. *Blood* 103:988–994.
13. Stonier SW, Ma LJ, Castillo EF, Schluns KS (2008) Dendritic cells drive memory CD8 T-cell homeostasis via IL-15 transpresentation. *Blood* 112:4546–4554.
14. Mortier E, et al. (2009) Macrophage- and dendritic-cell-derived interleukin-15 receptor alpha supports homeostasis of distinct CD8+ T cell subsets. *Immunity* 31: 811–822.
15. Mortier E, Woo T, Advincula R, Gozalo S, Ma A (2008) IL-15Ralpha chaperones IL-15 to stable dendritic cell membrane complexes that activate NK cells via trans presentation. *J Exp Med* 205:1213–1225.
16. Bergamaschi C, et al. (2012) Circulating IL-15 exists as heterodimeric complex with soluble IL-15Rα in human and mouse serum. *Blood* 120:e1–e8.
17. Anthony SM, Howard ME, Hailemichael Y, Overwijk WW, Schluns KS (2015) Soluble interleukin-15 complexes are generated in vivo by type I interferon dependent and independent pathways. *PLoS One* 10:e0120274.
18. Anthony SM, et al. (2016) Inflammatory signals regulate IL-15 in response to lymphodepletion. *J Immunol* 196:4544–4552.
19. Stoklasek TA, Schluns KS, Lefrançois L (2006) Combined IL-15/IL-15Ralpha immunotherapy maximizes IL-15 activity in vivo. *J Immunol* 177:6072–6080.
20. Rubinstein MP, et al. (2006) Converting IL-15 to a superagonist by binding to soluble IL-15Ralpha. *Proc Natl Acad Sci USA* 103:9166–9171.
21. Castillo EF, Stonier SW, Frasca L, Schluns KS (2009) Dendritic cells support the in vivo development and maintenance of NK cells via IL-15 trans-presentation. *J Immunol* 183:4948–4956.
22. Schluns KS, et al. (2004) Distinct cell types control lymphoid subset development by means of IL-15 and IL-15 receptor alpha expression. *Proc Natl Acad Sci USA* 101: 5616–5621.
23. Reinecker HC, MacDermott RP, Mirau S, Dignass A, Podolsky DK (1996) Intestinal epithelial cells both express and respond to interleukin 15. *Gastroenterology* 111: 1706–1713.
24. Ma LJ, Acero LF, Zal T, Schluns KS (2009) Trans-presentation of IL-15 by intestinal epithelial cells drives development of CD8alphaalpha IELs. *J Immunol* 183:1044–1054.
25. Castillo EF, Acero LF, Stonier SW, Zhou D, Schluns KS (2010) Thymic and peripheral microenvironments differentially mediate development and maturation of iNKT cells by IL-15 transpresentation. *Blood* 116:2494–2503.
26. Blauvelt A, et al. (1996) Interleukin-15 mRNA is expressed by human keratinocytes Langerhans cells, and blood-derived dendritic cells and is downregulated by ultraviolet B radiation. *J Invest Dermatol* 106:1047–1052.
27. Colpitts SL, et al. (2012) Cutting edge: The role of IFN-α receptor and MyD88 signaling in induction of IL-15 expression in vivo. *J Immunol* 188:2483–2487.
28. Colpitts SL, et al. (2013) Transcriptional regulation of IL-15 expression during hematopoiesis. *J Immunol* 191:3017–3024.
29. Sosinowski T, et al. (2013) CD8α+ dendritic cell trans presentation of IL-15 to naive CD8+ T cells produces antigen-inexperienced T cells in the periphery with memory phenotype and function. *J Immunol* 190:1936–1947.
30. Burkholder B, et al. (2014) Tumor-induced perturbations of cytokines and immune cell networks. *Biochim Biophys Acta* 1845:182–201.
31. Fuertes MB, et al. (2011) Host type I IFN signals are required for antitumor CD8+ T cell responses through CD8alpha+ dendritic cells. *J Exp Med* 208:2005–2016.
32. Zhang X, Sun S, Hwang I, Tough DF, Sprent J (1998) Potent and selective stimulation of memory-phenotype CD8+ T cells in vivo by IL-15. *Immunity* 8:591–599.
33. Soudja SM, Ruiz AL, Marie JC, Lauvau G (2012) Inflammatory monocytes activate memory CD8(+) T and innate NK lymphocytes independent of cognate antigen during microbial pathogen invasion. *Immunity* 37:549–562.
34. Deng L, et al. (2014) STING-dependent cytosolic DNA sensing promotes radiation-induced type I interferon-dependent antitumor immunity in immunogenic tumors. *Immunity* 41:843–852.
35. Woo SR, et al. (2014) STING-dependent cytosolic DNA sensing mediates innate immune recognition of immunogenic tumors. *Immunity* 41:830–842.
36. Demaria O, et al. (2015) STING activation of tumor endothelial cells initiates spontaneous and therapeutic antitumor immunity. *Proc Natl Acad Sci USA* 112: 15408–15413.
37. Corrales L, et al. (2015) Direct activation of STING in the tumor microenvironment leads to potent and systemic tumor regression and immunity. *Cell Rep* 11:1018–1030.
38. Lebrec H, et al. (2013) Homeostasis of human NK cells is not IL-15 dependent. *J Immunol* 191:5551–5558.
39. Lodolce JP, et al. (1998) IL-15 receptor maintains lymphoid homeostasis by supporting lymphocyte homing and proliferation. *Immunity* 9:669–676.
40. Richer MJ, et al. (2015) Inflammatory IL-15 is required for optimal memory T cell responses. *J Clin Invest* 125:3477–3490.
41. Liu RB, et al. (2013) IL-15 in tumor microenvironment causes rejection of large established tumors by T cells in a noncognate T cell receptor-dependent manner. *Proc Natl Acad Sci USA* 110:8158–8163.
42. Bamford RN, Battiata AP, Waldmann TA (1996) IL-15: The role of translational regulation in their expression. *J Leukoc Biol* 59:476–480.
43. Engblom C, Pfirschke C, Pittet MJ (2016) The role of myeloid cells in cancer therapies. *Nat Rev Cancer* 16:447–462.
44. Kluger HM, et al. (2015) Characterization of PD-L1 expression and associated T-cell infiltrates in metastatic melanoma samples from variable anatomic sites. *Clin Cancer Res* 21:3052–3060.
45. Tough DF, Borrow P, Sprent J (1996) Induction of bystander T cell proliferation by viruses and type I interferon in vivo. *Science* 272:1947–1950.
46. Stoklasek TA, Colpitts SL, Smilowitz HM, Lefrancois L (2010) MHC class I and TCR avidity control the CD8 T cell response to IL-15/IL-15Rα complex. *J Immunol* 185: 6857–6865.
47. Kawamura T, Koka R, Ma A, Kumar V (2003) Differential roles for IL-15R alpha-chain in NK cell development and Ly-49 induction. *J Immunol* 171:5085–5090.
48. Caton ML, Smith-Raska MR, Reizis B (2007) Notch-RBP-J signaling controls the homeostasis of CD8- dendritic cells in the spleen. *J Exp Med* 204:1653–1664.
49. Clausen BE, Burkhardt C, Reith W, Renkawitz R, Förster I (1999) Conditional gene targeting in macrophages and granulocytes using LysMcre mice. *Transgenic Res* 8: 265–277.
50. Sauer JD, et al. (2011) The N-ethyl-N-nitrosourea-induced Goldenticket mouse mutant reveals an essential function of Sting in the in vivo interferon response to Listeria monocytogenes and cyclic dinucleotides. *Infect Immun* 79:688–694.
51. Hohl TM, et al. (2009) Inflammatory monocytes facilitate adaptive CD4 T cell responses during respiratory fungal infection. *Cell Host Microbe* 6:470–481.
52. Müller U, et al. (1994) Functional role of type I and type II interferons in antiviral defense. *Science* 264:1918–1921.
53. Saederup N, et al. (2010) Selective chemokine receptor usage by central nervous system myeloid cells in CCR2-red fluorescent protein knock-in mice. *PLoS One* 5: e13693.